Binocular temporal visual processing in myopia

Fuensanta A. Vera-Diaz New England College of Optometry, Boston, MA, USA

Peter J. Bex Northeastern University, Boston, MA, USA

Adriana Ferreira New England College of Optometry, Boston, MA, USA

Anna Kosovicheva Northeastern University, Boston, MA, USA

Our ability to utilize binocular visual information depends on the visibility of the retinal images in each eye, which varies with both their spatial and temporal frequency content. Although the effects of spatial information on binocular function have been established, the effects of temporal frequency on binocularity are less well understood. These factors may also vary with refractive error if spatiotemporal sensitivity is affected by structural changes during the emmetropization process that may differentially affect distinct ganglion cells. In a cross-sectional study, we evaluated the potential effects of temporal and spatial frequency on binocularity in young individuals with emmetropia or myopia. Stereopsis and binocular balance were measured as a function of temporal (0–12 Hz) and spatial (1–8 c/deg) frequency. Stereopsis thresholds were measured by determining the minimum disparity at which subjects accurately identified the depth of bandpass-filtered rings. Binocular balance was measured by determining the relative contrast at which subjects reported dichoptic bandpass-filtered letters with equal frequency. Stereopsis thresholds were temporal but not spatial frequency dependent whereas binocular balance was spatial and temporal frequency dependent. There were no differences in monocular spatiotemporal contrast sensitivity between refractive groups in our sample. However, individuals with myopia showed reduced stereopsis with flickering stimuli and greater binocular imbalance at higher spatial and lower temporal frequencies compared to emmetropes. Differences in *binocular* vision between emmetropia and corrected myopia depend on temporal as well as spatial frequency and may be the cause or consequence of abnormal emmetropization during visual development.

Introduction

Binocular vision is important for our interaction with the environment, providing the visual system with information about the three-dimensional structure of the world. Our ability to utilize stereoscopic depth information depends on the degree of sensitivity to the temporal and spatial frequency content of the retinal images in both eyes (Kelly, 1971; Robson, 1966). The influence of spatial factors in binocular visual function has been well documented. For example, retinal image focus and spatial frequency content influence binocular matching (Hoffman & Banks, 2010), binocular rivalry (Fahle, 1982, 1983; Shors, Wright, & Greene, 1992), and stereoacuity (Schor & Wood, 1983; Westheimer & McKee, 1980; Yang & Blake, 1991).

In comparison, less is known about the interactions between temporal visual information and binocular vision. Stereopsis thresholds have been shown to depend on the temporal frequency of luminance modulation when measured with flickering or drifting luminance-defined gratings (S. Lee, Shioiri, & Yaguchi, 2003, 2007; Patterson, 1990). These experiments have shown that stereoacuity is impaired at high temporal frequencies, particularly when the spatial frequency is high. Stereopsis thresholds also depend on temporal modulations in the disparity signal itself when measured with disparity-defined targets (Kane, Guan, & Banks, 2014; Nienborg, Bridge, Parker, & Cumming, 2005; Norcia & Tyler, 1984; Richards, 1972). These experiments have shown a much more limited spatial and temporal envelope of disparity sensitivity with a high temporal frequency cutoff typically between 6 and 12 Hz. This variation in sensitivity is likely the product of spatiotemporal windowing used to estimate binocular disparity (Kane et al., 2014).

Temporal information also plays a role in other binocular interactions, including binocular summation and interocular suppression. For example, binocular summation is largest when dichoptic stimuli are closely spaced in time (Matin, 1962; Thorn & Boynton, 1974) and has been shown to depend on the similarity in

Citation: Vera-Diaz, F. A., Bex, P. J., Ferreira, A., & Kosovicheva, A. (2018). Binocular temporal visual processing in myopia. *Journal of Vision*, *18*(11):17, 1–12, https://doi.org/10.1167/18.11.17.

https://doi.org/10.1167/18.11.17 Received January 15, 2018; published October 29, 2018 ISSN 1534-7362

temporal frequency and phase between the two eyes (Blake & Rush, 1980; Cavonius, 1979). In contrast, when a flickering image is presented to one eye and a different static image to the other eye, the flickering image dominates perception (Kaunitz, Fracasso, Skujevskis, & Melcher, 2014; Tsuchiya & Koch, 2005; Tsuchiya, Koch, Gilroy, & Blake, 2006). This effect, known as continuous flash suppression, is frequently used to study attention selection and is temporal frequency dependent (Han & Alais, 2018; Han, Lunghi, & Alais, 2016; Tsuchiya & Koch, 2005; W. Zhu, Drewes, & Melcher, 2016). Less is known about the temporal dependence of binocular balance when the two different images flicker at the same frequency.

These effects of spatial and temporal image content on binocularity may further interact with refractive error. The development of different aspects of temporal vision varies with age with sensitivity to low temporal frequencies maturing later in childhood (Banks, 1982; Dobkins, Anderson, & Lia, 1999; Ellemberg, Lewis, Liu, & Maurer, 1999; Hartmann & Banks, 1992; Stavros & Kiorpes, 2008). Retinal image content provides an important visual feedback signal for eye growth control during the emmetropization process (Goss & Wickham, 1995; Hess, Schmid, Dumoulin, Field, & Brinkworth, 2006; Smith, Hung, & Arumugam, 2014; Wallman & Winawer, 2004). Therefore, abnormal development of temporal as well as spatial vision may affect the ability to process and use visual information and interfere with normal emmetropization. However, data on the relationship between refractive error and sensitivity to temporal visual information is very limited. Two previous studies, Ong and Wong (1971) and Chen, Woung, and Yang (2000), found decreased critical flicker frequencies (CFFs) in subjects with high myopia without a clear correlation between the reduction in CFF and the magnitude of myopia. On the other hand, Comerford, Thorn, and Corwin (1987) found no effect of high refractive errors on the temporal contrast sensitivity function (tCSF). The tCSF of individuals with low-to-moderate myopia has not previously been reported.

In addition to these effects of myopia on monocular processing of temporal visual information, there are limited data on the role of binocularity and temporal vision in refractive error development. Binocular vision depends on the visibility of the retinal images in each eye, which, in turn, varies with their spatial and temporal frequency content. These factors may also vary with refractive error if spatiotemporal sensitivity is affected by structural changes in the eye during the emmetropization process. There are many classes of retinal ganglion cell that differ in their morphology and functional selectivity (for review, see Sanes & Masland, 2015). These structural differences mean that different ganglion cell types may be differently affected by the elongation of the eye in myopia.

In this study, we aimed to measure the temporal frequency (TF) dependence of binocular vision as a function of spatial frequency (SF) in young adults. It is thought that low spatial and high temporal frequencies are selectively processed by magnocellular retinal ganglion cell pathways whereas high spatial and low temporal frequencies may be selectively processed by parvocellular retinal ganglion cell pathways (for review, see Nassi & Callaway, 2009), and differences in the morphology of these cells may lead to differences in their sensitivity as a consequence of eye elongation in myopia (Vera-Diaz, McGraw, Strang, & Whitaker, 2005). We used two forced-choice tasks to measure binocularity as a function of spatial and temporal frequency: binocular balance and stereopsis thresholds. We hypothesize an effect of temporal and spatial frequency on binocularity measures.

Methods

Subjects

A total of 33 young adult subjects (mean ± *SD* age: 24.6 ± 1.85 years) were recruited from the student population of the New England College of Optometry to participate in this study. Following a vision screening that comprised an ocular history questionnaire and ocular heath evaluation, subjects who met all inclusion criteria were enrolled in the study. Criteria for subjects' inclusion were: (a) within 18–31 years of age; (b) best corrected visual acuity (BCVA) 20/20 or better in each eye; (c) refractive error (spherical equivalent, SE) between +0.75 hyperopia and −8.00DS myopia with ≤1.50DC of astigmatism or ≤1.00D anisometropia; (d) no current binocular vision or accommodative dysfunction; (e) not using any medications that may affect their vision; (f) no history of surgery or eye disease that may have resulted in visual consequences; and (g) adequate hearing, language skills, and mental ability to understand the consent process and the instructions given during the experiment.

Subjects' refractive errors for each eye were determined by objective refraction with an open-field autorefractor (Grand Seiko WR5100K, http://www.grandseiko.com) followed by binocular subjective refraction with binocular balancing and evaluated by the observer's BCVA with a computerized LogMAR chart. Axial length measurements were performed with a Haag-Streit Lenstar LS900 optical biometer (http://www.haag-streit.com/). Subjects were grouped based on their refractive error. Myopia ($n = 14$) was defined as an SE in each eye between −0.75DS and −8.00DS (Mean: −3.45 ± 2.10DS). Emmetropia ($n = 19$) was defined as SE in each eye between −0.25DS and

+0.75DS (Mean: +0.27 ± 0.29DS). Power vector analyses of the spherocylindrical refractive error were calculated (Thibos & Horner, 2001). Each subject's refractive error was represented by three values (M, J_0, and J_{45}), where M corresponds to the spherical equivalent power and J_0 and J_{45} correspond to the cylinder power at axis 0° and 45°, respectively. An additional motor eye dominance test (hole in card; Pointer, 2012; Walls, 1951) was performed.

This research followed the tenets of the Declaration of Helsinki; informed consent was obtained from all subjects after explanation of the nature and possible consequences of the study and was approved by the New England College of Optometry's institutional review board.

Display, stimuli, and procedures

The experiment was programmed with the Psychophysics Toolbox Version 3 (Brainard, 1997; Kleiner, Brainard, & Pelli, 2007; Pelli, 1997) in MATLAB (MathWorks, Natick, MA). Stimuli were presented on a gamma-corrected ROG SWIFT PG278Q Asus monitor with a resolution of 1,920 × 1,080 pixels (display dot pitch 0.233 mm) running at 120 Hz from an NVidia GeForce GTX 780 graphics-processing unit. The response of the display was measured with an optical transient recorder OTR–3 (Display Metrology & Systems GmbH & Co. KG, Karlsruhe, Germany).

Subjects were seated 40 cm in front of the monitor that subtended 73° by 46° of visual angle with their heads stabilized in a chin and forehead rest. Force-choice tasks were used to measure, in the same order for all subjects, (a) stereopsis and (b) binocular balance as a function of temporal and spatial frequency. Subjects viewed the display binocularly through wireless LCD active shutter glasses (NVidia 3D Vision, http://www.nvidia.com; 60 Hz monocular refresh). Binocular balance stimuli consisted of spatially bandpass-filtered Sloan letters with a 5:1 optotype height-to-stroke width ratio. Stereopsis stimuli consisted of circles with a 1:1 aspect ratio. Both types of stimuli were shown on a uniform gray (85 cd/m^2) background. All images were spatially filtered using an isotropic log exponential filter with a bandwidth (full width at half maximum) of two octaves. The peak spatial frequency was fixed at five cycles per image, corresponding to the spatial scale for peak letter identification (J. A. Solomon & Pelli, 1994). Images were scaled to 5°, 2.5°, 1.25°, and 0.625° in height. The resulting images had peak spatial frequencies of 1, 2, 4, and 8 c/deg, respectively. Temporal frequency was manipulated in separate blocks of trials, using sinusoidal counterphase flicker at one of four frequencies; 0 (static), 4, 7.5, and 12 Hz.

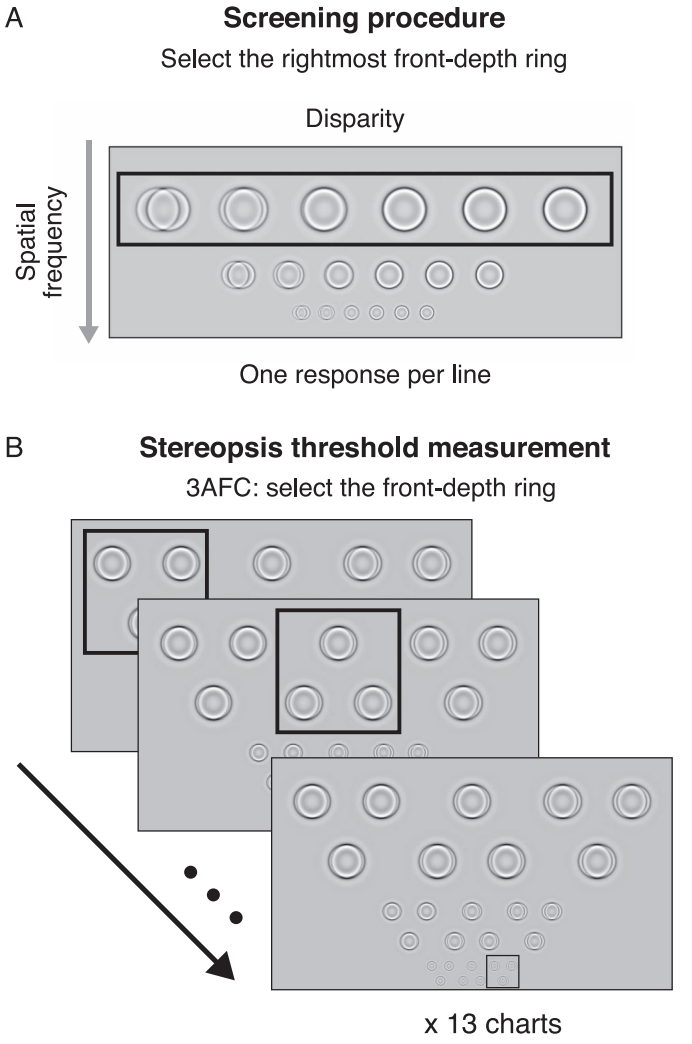

Figure 1. (A) Screening stimuli used to determine the starting point for the staircases in the stereopsis threshold task. Circles were arranged in order of decreasing disparity from left to right (all front depth). For each line, subjects selected the rightmost circle (smallest disparity) that appeared to have front depth. (B) Stimuli used for the stereopsis thresholds task. Each triplet consisted of one randomly selected front-depth circle and two back-depth circles, and subjects were instructed to identify the front-depth circle by clicking on it. For ill7ustrative purposes, only three spatial frequency conditions (three stimulus rows) are shown. Left- and right-eye views are superimposed to show the degree of binocular disparity.

Stereopsis

The stimuli used to measure stereoscopic disparity thresholds were arranged into charts (Figure 1B and Supplementary Movie S1), each consisting of stereoscopic circles grouped into 12 triplets. Each triplet consisted of two randomly selected elements with uncrossed disparity (behind the screen) and one randomly selected element with crossed disparity (in front of the screen). Crossed and uncrossed disparities were produced by equal but opposite horizontal

displacements of the left- and right-eye images by half the total disparity. The absolute disparity was the same for each circle within the triplet. In the flicker conditions, all circles within a chart flickered at the same temporal frequency, and each triplet was assigned a randomly selected phase. All circles within a triplet were identical in phase with no temporal lag between the images in the two eyes. Peak Michelson contrast for each circle was 100%. Charts were organized into four lines, each line containing three triplets from a single spatial frequency condition (Figure 1B). The four lines were arranged in order of increasing spatial frequency from the top to the bottom of the display. Triplets were arranged in triangular configurations with equal spacing between each pair of circles (center-to-center separation of 2.2 times the circle height). The horizontal center-to-center separation between adjacent triplets was equal to four times the individual circle height in that line. Vertical center-to-center spacing between adjacent lines was set to four times the circle height on the upper line. Within a row, triplets alternated between downward- and upward-pointing triangular configurations as shown in Figure 1B.

Subjects performed a three-alternative, forced-choice (3AFC) task in which they were instructed to click on the front-depth circle within each triplet using a cursor, guessing if necessary, moving from left to right within each line and top to bottom on the chart. Subjects viewed the charts freely and were given unlimited time to respond. The triplet to which the subject was required to respond on a given trial was centered within a black Nonius box ($\approx$0 cd/m^2), 2.15 times the height and width of an individual circle on that line and a stroke width of 0.05 times the circle height. This frame was introduced to facilitate binocular fusion and to highlight the subject's progress. Once the subject clicked on a circle within a triplet, the Nonius box moved to the next triplet on the chart.

Stereopsis thresholds were quantified by determining the minimum binocular disparity at which the subject identified the front-depth target with 75% accuracy. Within a block of trials, disparity was controlled using a QUEST staircase algorithm (Watson & Pelli, 1983). The disparity levels were controlled by four simultaneous, independent QUEST staircases with one staircase for each spatial frequency condition. Disparity test levels were updated one chart at a time, taking into account responses from all preceding charts within a block of trials. Within each row, the disparities for each triplet were equal to the peak, +2 and −2 standard deviation of the current QUEST threshold estimate for each spatial frequency condition, arranged in a random order.

To improve the efficiency of the test, the starting disparity level for each staircase was established by a screening procedure at the beginning of each block of trials. Subjects were shown a chart consisting of 24 individual stereoscopic front-depth circles, arranged in four lines, corresponding to each of the four spatial frequency conditions (Figure 1A). For each individual line, starting from the top, subjects were instructed to click on the rightmost circle that still appeared to be just in front of the display. The disparity of this target was used as the starting point of the QUEST staircase for the corresponding spatial frequency in the main experiment. Within each line, six circles were organized in order of decreasing disparity from left to right in logarithmic steps. The rightmost circle of each line had a disparity of 38.6 arcsec, and the leftmost circle had a disparity of either 3,750, 2,193, 1,268, or 717 arcsec for the 1, 2, 4, and 8 c/deg conditions, respectively. Circles within a row had a horizontal center-to-center spacing of twice the circle height, and pairs of adjacent lines had a vertical center-to-center separation of 1.5 times the circle height for the upper line. The line to which the subject was currently responding was framed by a rectangle 12.31 times the width and 2.31 times the height of an individual circle in the corresponding line (thickness scaled to 0.05 times the circle height). After each response, the rectangle moved to highlight the line immediately below it.

Following the screening procedure, subjects completed 13 charts (39 trials for each spatial frequency condition). The four temporal frequency conditions (0, 4, 7.5, and 12 Hz) were completed in separate blocks of trials in a random order for each subject. Subjects completed a total of 624 trials (39 trials for each unique combination of spatial and temporal frequency condition).

Binocular balance

Stimuli and procedures for the binocular balance measurements were based on the dichoptic letter procedure to measure interocular contrast ratios described by Kwon, Wiecek, Dakin, and Bex (2015; Figure 2A and Supplementary Movie S2). Each letter chart consisted of 40 Sloan letters that were grouped into 20 spatially overlapping dichoptic pairs, which were arranged into four lines. Each line consisted of five letters from a single spatial frequency condition, and the four lines were arranged in order of increasing spatial frequency from top to bottom. Letters within a given line were evenly spaced with a horizontal center-to-center separation of twice the letter height in the corresponding line. Vertical center-to-center spacing between adjacent lines was set to 1.5 times the letter height on the upper of the two lines. Letters for each line were selected by drawing 10 random letters without replacement from the full set of 26 letters of the alphabet, which were then arranged into five pairs. To promote stable ocular vergence, the entire chart was

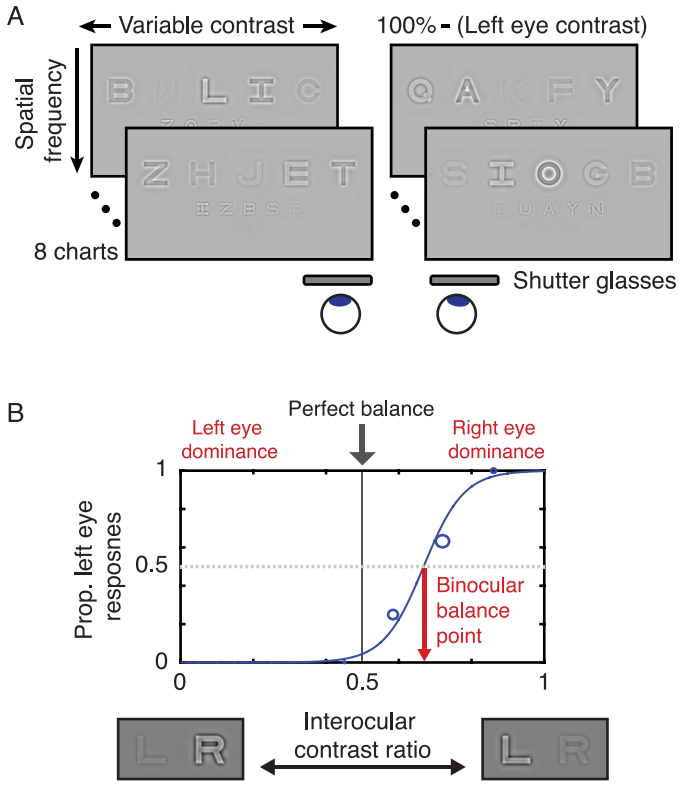

Figure 2. (A) Stimuli used for the binocular balance task. Subjects viewed dichoptic letter charts and read the letters from left to right, reporting the dominant percept for each letter in a 2AFC task. Interocular contrast was varied to determine the binocular balance point—the contrast level at which the two letters were reported with equal frequency. Stimulus contrast in the right eye was set to 100% minus the contrast in the left eye. (B) The proportion of responses corresponding to the letter shown in the left eye is plotted as a function of the interocular contrast ratio for one subject, where 0 corresponds to 0% left-eye contrast, and 1 corresponds to 100% left-eye contrast. The magnitude of binocular balance was estimated as the absolute difference of the interocular contrast ratio (at the binocular balance point, red arrow) from equal contrast (0.5) in each eye.

surrounded by a binocular, screen-centered black rectangular Nonius frame (52.20° width × 20.95° height, line width: 0.55°). The entire chart was continuously visible, and subjects viewed the display freely. Subjects performed a 2AFC task (the two letters shown to the two eyes) for each dichoptic letter pair. They were instructed to report the dominant percept by reading the letters on the chart out loud from left to right, top to bottom.

The magnitude of binocular balance was quantified by varying the relative contrast of the letters in each dichoptic pair to find the interocular balance point, defined as the relative contrast at which subjects reported the two letters within a pair with equal frequency (Figure 2B). The contrast levels were constrained within a given letter pair, such that the peak Michelson contrast of the letter in the right eye was always 100% minus the peak Michelson contrast of the letter in the left eye. Similar to the stereopsis task, contrast levels were controlled by four simultaneous but independent QUEST staircases (Watson & Pelli, 1983), one for each line, set to converge on an equal proportion (50%) of left- and right-eye responses. On the first chart, the contrast levels on each line were fixed at five linearly spaced levels from 10% to 90% contrast in the left eye. On each subsequent chart, the five contrast levels were calculated from the peak, +1, +2, −1, and −2 standard deviations of the current QUEST threshold estimate. The five contrast levels for each line were always randomly assigned to one of the five letter positions. As with the other tasks, contrast levels were updated one chart at a time, taking into account responses from all preceding charts within a block of trials. Subjects were given unlimited time to respond, and responses were entered by the experimenter using a keyboard.

Four temporal frequency conditions were completed in a random order and in separate blocks of trials. All letters within a chart flickered at the same temporal frequency with a randomly selected phase for each individual letter. The independent selection of phases for each letter within a pair resulted in a net absence of any temporal delays between the two eyes. Each block consisted of eight charts with a total of 160 dichoptic letter pairs across all four lines. Therefore, each subject completed 40 trials (i.e., letter pairs) for each unique combination of spatial frequency and temporal frequency condition, 640 trials in total.

To test whether potential differences in binocularity were caused by monocular differences in temporal vision, monocular temporal CSF measurements were taken for all subjects. The area under the log temporal CSF (AULTCSF) and the CFF threshold were used to determine monocular temporal contrast sensitivity (see Supplementary Appendix S1 for a detailed description of the tCSF procedure and results).

Data analysis

Stereopsis thresholds and binocular balance points were calculated by fitting the staircase data to a two-parameter logistic function using maximum likelihood estimation (α: threshold, β: slope). The 75% and 50% thresholds were calculated from the resulting fits for both the stereoacuity and balance point estimates, respectively. The magnitude of binocular balance was estimated as the absolute difference of the interocular contrast ratio (corresponding to the 50% threshold) from equal contrast (0.5) in each eye (Figure 2B). For calculating stereopsis thresholds, disparity values were converted to $\log_{10}$ units prior to curve fitting and

statistical analysis. Statistical comparisons were performed using a 4 (peak SF) × 4 (TF) × 2 (refractive error group) mixed-model ANOVA using the Satterthwaite approximation for denominator degrees of freedom. SF and TF were within-subject factors and refractive error group was a between-subjects factor.

In the stereopsis data, the 1 c/deg spatial frequency condition was removed from the analysis for all subjects due to high variability of subject responses and reported difficulty with the test (across all subjects, 33.3%, or 44 out of 132 observations, had an overall accuracy of 50% or less). Stereopsis threshold values for a given subject and stimulus condition were otherwise removed from the analysis if they met at least one of the following criteria: no stereopsis in the screening procedure, fitted thresholds >5,000 arcsec, or overall proportion correct not significantly better than chance (using a binomial test), resulting in the removal of 14.1% of the remaining observations. Relationships between refractive error (spherical equivalent, averaged across the two eyes), axial length, and the two binocularity measures were quantified using Spearman's rank correlation coefficient. Unless otherwise noted, correlation coefficients for the two binocularity measures were calculated from averaged values across all conditions to produce one observation per subject.

The complete data set is available on the Open Science Framework online (https://osf.io/7hx9v).

Results

Stereopsis

Figure 3A shows mean stereopsis thresholds at each spatial and temporal frequency condition, separately for the groups of subjects with myopia and emmetropia. A three-way mixed ANOVA on stereopsis thresholds with two refractive error groups (myopia and emmetropia), three SFs and four TFs showed no main effect of refractive group, $F(1, 29.86) = 3.29$, $p = 0.08$, but a significant main effect of temporal frequency, $F(3, 77.24) = 7.48$, $p < 0.01$. These effects were qualified by a significant TF × refractive group interaction, $F(3, 77.24) = 4.92$, $p < 0.01$, with myopes showing higher stereopsis thresholds (i.e., reduced stereoacuity) compared with emmetropes at temporal frequencies above 0 Hz (Figures 3B and 4A).

Pairwise post hoc contrasts between myopes and emmetropes at each of the four TFs showed that this difference was only significant at 4 Hz, $t(44.74) = 3.12$, $p = 0.003$, with a Bonferroni-corrected alpha (α_B) of 0.0125 (all other p-values > 0.13). There was no main effect of spatial frequency, $F(2, 55.75) = 2.46$, $p = 0.09$, or interaction between SF and refractive group, $F(2, 55.75) = 2.82$, $p = 0.07$. Neither the SF × group interaction nor the three-way TF × SF × refractive group interaction were significant (p-values > 0.17).

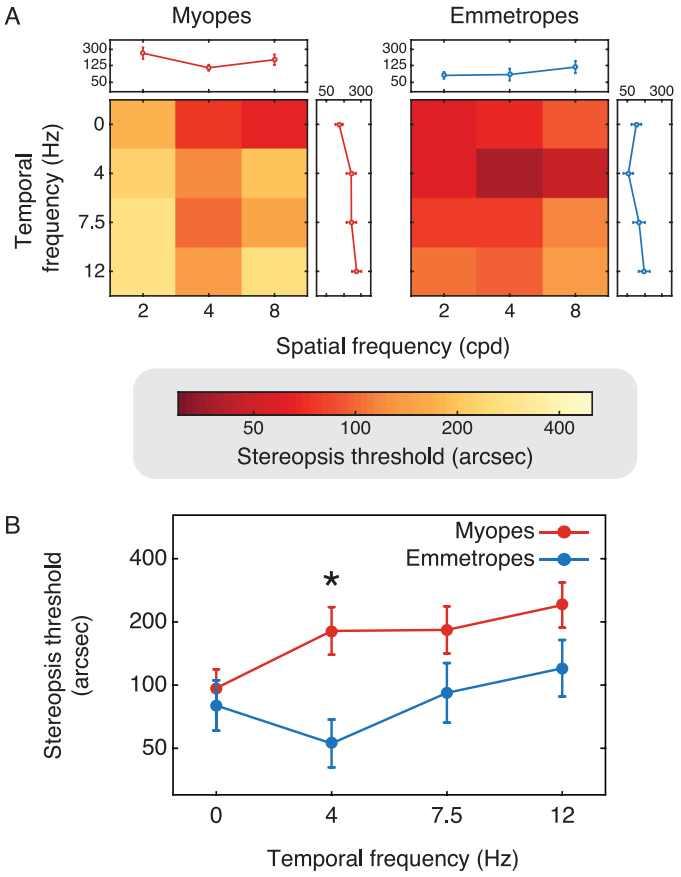

Figure 3. (A) Mean stereopsis thresholds as a function of the letter's peak spatial and temporal frequency for individuals with myopia (left panel) and emmetropia (right panel). Side panels in panel A show thresholds collapsed across temporal or spatial frequency conditions (top and right panels, respectively). Error bars in the linear graphs show ±1 standard error. (B) Mean stereopsis thresholds (arcsec) for myopes (red) and emmetropes (blue) at each temporal frequency condition, averaged across spatial frequencies. *Significance with a Bonferroni correction for four comparisons ($\alpha_B = 0.0125$).

There was a significant negative correlation between refractive error and stereoacuity with subjects with higher myopia (negative refractive error) showing higher stereopsis thresholds, $r_s(31) = -0.37$, $p = 0.04$. Given the significant TF × group interaction, we separately calculated this correlation at each temporal frequency (averaged across all spatial frequencies). As shown in Figure 4B, these results were similar to the pairwise comparisons between groups with a significant correlation only at 4 Hz, $r_s(31) = -0.55$, $p = 0.001$, $\alpha_B = 0.0125$, all other p-values > 0.05. Axial length was not significantly correlated with stereopsis thresholds, $r_s(31) = 0.23$, $p = 0.2$.

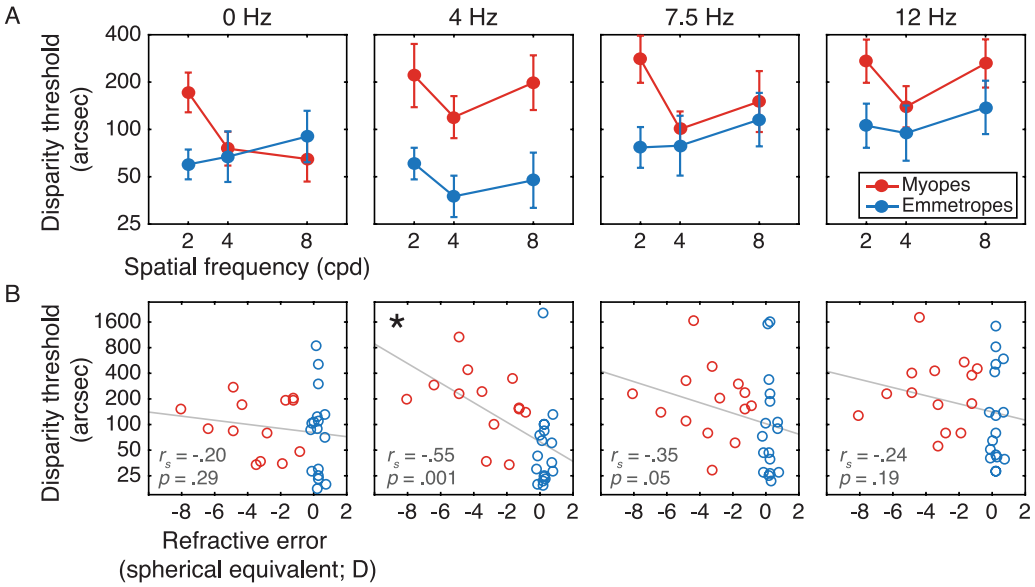

Figure 4. (A) Mean stereopsis thresholds for myopes (red) and emmetropes (blue) as a function of spatial frequency with each panel showing one temporal frequency condition. (B) Correlation between refractive error (mean M for both eyes, D) and mean stereopsis thresholds (arcsec) for individuals with myopia (red) and emmetropia (blue), calculated separately at each temporal frequency. Error bars show ±1 standard error. *Significance with a Bonferroni correction for four comparisons ($\alpha_B = 0.0125$).

Stereoacuity measured with the Random Dot 3 clinical test was significantly correlated with our stereopsis thresholds, $r_s(31) = 0.39$, $p = 0.03$.

Binocular balance

Figure 5A shows mean binocular balance values at each spatial and temporal frequency condition, separately for the two refractive error groups, where larger values denote greater interocular suppression. A three-way mixed ANOVA on binocular balance with two refractive error groups (myopia and emmetropia), four SFs, and four TFs showed no significant main effect of refractive group, $F(1, 31) = 0.78$, $p = 0.38$. There was also no main effect of temporal frequency, $F(3, 93) = 2.29$, $p = 0.08$; however, there was a significant main effect of spatial frequency, $F(3, 93) = 6.21$, $p < 0.01$. These effects were qualified by a significant three-way SF × TF × refractive group interaction, $F(9, 279) = 2.47$, $p = 0.01$, with myopes showing more binocular imbalance compared with emmetropes, particularly at higher SFs and lower TFs (Figure 5A, upper-right corner). No other interactions were significant (all p-values > 0.14).

There was no significant correlation between the amount of refractive error and binocular balance, $r_s(31) = 0.08$, $p = 0.65$ (Figure 5B). As expected, the degree of binocular imbalance was very small (<13%) compared with levels found in amblyopic subjects (Birch et al., 2016; Kwon et al., 2014; Kwon et al., 2015).

Monocular temporal contrast sensitivity

The full results of the temporal contrast sensitivity measurement are described in Supplementary Appendix S1. Briefly, we found no significant differences between emmetropes and myopes in either the AULTCSF, $F(1, 30.96) = 3.21$, $p = 0.08$, or CFF, $F(1, 31.13) = 3.75$, $p = 0.06$. In addition, neither AULTCSF, $r_s(31) = -0.07$, $p = 0.72$, nor CFF, $r_s(31) = -0.2$, $p = 0.28$, were correlated with stereopsis thresholds nor with the level of binocular balance: $r_s(31) = -0.04$, $p = 0.81$ for AULTCSF; $r_s(31) = -0.18$, $p = 0.31$ for CFF. The difference in AULTCSF between the dominant and nondominant eyes was also not correlated with the level of binocular balance, $r_s(31) = -0.26$, $p = 0.15$, nor with stereopsis thresholds, $r_s(31) = -0.06$, $p = 0.76$.

Discussion

We found dissimilar effects of temporal and spatial frequency on two binocular visual function tasks in a group of young adults, indicating that these two tasks evaluate different aspects of visual processing. Across both refractive groups, the pattern of stereopsis thresholds was consistent with previously reported results using temporal luminance modulations, demonstrating elevated thresholds at high temporal frequencies (S. Lee et al., 2003, 2007; Patterson, 1990). As expected, the observed spatial and temporal variation in thresholds is somewhat lower than that reported in experiments varying the spatial and

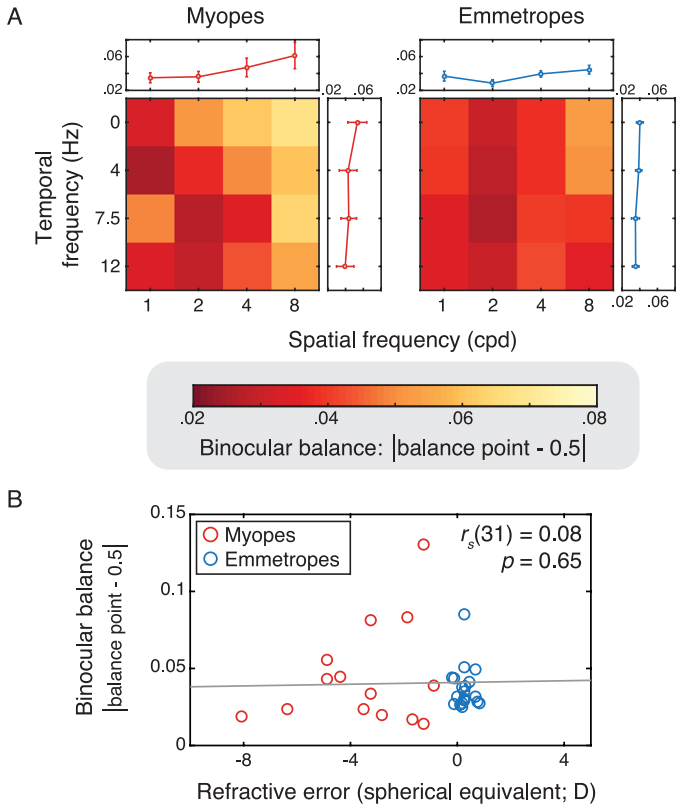

Figure 5. (A) Mean binocular balance values for subjects with myopia (left panel) and emmetropia (right panel) as a function of the letter's peak spatial frequency and temporal frequency. Larger values correspond to greater interocular suppression. Side panels in panel A show binocular balance values collapsed across temporal or spatial frequency conditions (top and right panels, respectively). Error bars in the linear graphs show ±1 standard error. (B) Correlation between refractive error (mean M for both eyes, D) and binocular balance values. Each scatter point represents one subject (average of 16 observations across spatial and temporal frequency conditions) with red scatter points corresponding to myopes and blue points corresponding to emmetropes.

temporal profile of the disparity information (Kane et al., 2014; Norcia & Tyler, 1984; Richards, 1972). In contrast to the observed increase in stereopsis thresholds at high temporal frequencies, we observed greater degrees of binocular imbalance (i.e., greater interocular suppression) at low temporal frequencies and mid to high spatial frequencies, particularly in myopes. The increase at higher spatial frequencies is consistent with previous results in subjects with amblyopia (Birch et al., 2016; Kwon et al., 2015). Although comparable binocular balance estimates have not been previously reported with binocular flicker, the increase at low temporal frequencies is consistent with recent evidence that continuous flash suppression may be strongest at low temporal frequencies (Han et al., 2016).

Previous work has indicated that binocular rivalry and stereopsis likely share common neural mechanisms (Harrad, McKee, Blake, & Yang, 1994; Hochberg, 1964), which would predict similar patterns of spatial and temporal frequency dependence for the two measures. In contrast, the differences between stereopsis and rivalry observed in our study may point to different spatial and temporal frequency ranges for the two phenomena. Although the underlying mechanisms for these differences have yet to be determined, previous work has shown that the two phenomena can be dissociated under specific conditions. For example, stereopsis and rivalry can co-occur within the same image (Julesz & Miller, 1975; Ogle & Wakefield, 1967).

We also found that these spatial and temporal factors in binocular visual processing interact with refractive error. Both refractive groups had monocular and binocular visual acuity that was optically corrected to 0.0 logMAR or better and had little to no interocular difference in acuity (32 subjects had an interocular difference in BCVA of 0.00 logMAR, and one subject had a difference of 0.1 logMAR). Subjects also showed similar monocular temporal contrast sensitivity results, which were not associated with either of the two binocular measures (see Supplementary Figure S4 in Supplementary Appendix S2). Nevertheless, statistically significant differences were found between our sample of subjects with emmetropia and myopia in the temporal frequency dependence of stereopsis and the spatial and temporal frequency dependence of binocular balance. Compared with subjects with emmetropia, those with myopia showed greater degrees of binocular imbalance at mid to high spatial frequencies and low temporal frequencies. In addition, stereopsis thresholds in myopes were larger with flickering stimuli with the largest difference observed at 4 Hz.

Neither of these effects could be attributed to monocular differences in temporal contrast sensitivity, which were not significantly different between individuals with emmetropia and myopia and, therefore, identify binocular vision processing effects. We additionally examined the potential presence of binocular visual deficits associated with small degrees of anisometropia (<1.0D) and astigmatism (<1.50D) on our binocular balance and stereopsis threshold estimates. Previous work has shown that a small percentage of individuals with these levels of anisometropia and astigmatism can exhibit monofixation or amblyopia (Weakley, 2001) although the incidence is greater in individuals with hyperopia than myopia (Kulp et al., 2014; C. E. Lee, Lee, & Lee, 2010; Weakley, 2001). Nonetheless, additional analyses showed no association between anisometropia, astigmatism, or anisoastigmatism and either of the two binocular measures (see Supplementary Figure S5 in Supplementary Appendix S2).

The optically corrected subjects with low-to-moderate myopia in our study showed comparable CFFs and AULTCSFs to those with emmetropia in agreement with previous studies (Comerford et al., 1987) and in contrast with other results showing lower CFFs in subjects with high myopia (>8.00DS; Chen et al., 2000; Ong & Wong, 1971). However, it is worth noting that these studies used large field luminance flicker to measure CFF, which has broad spatial frequency content that is dominated by low spatial frequencies (Burton & Moorhead, 1987; Field, 1987; Kretzmer, 1952). In our study, we used contrast-reversing flicker at a range of narrow-band spatial frequencies with no change in mean luminance over time.

In animal models, the temporal integration of spatial signals (e.g., hyperopic/myopic defocus) is nonlinear (for a review, see X. Zhu, McBrien, Smith, Troilo, & Wallman, 2013). This nonlinearity highlights the complexities of translating optical correction results of animal models to humans. For example, emmetropization in guinea pigs is dependent on specific temporal and spatial stimulus content with temporal frequencies of 7 Hz giving strongest signals for emmetropization (Zhi et al., 2013). The retinal circuit processing hyperopic defocus in chicks has also been found to depend on temporal characteristics (Schwahn & Schaeffel, 1997) although illuminance rich in blue light, such as sunlight, may protect against this effect (Rucker, Britton, Spatcher, & Hanowsky, 2015).

The potential effect of temporal frequency on subjects' binocularity and their ability to perceive depth may be consistent with previously suggested deficits in the magnocellular pathway in myopia (Ohlendorf & Schaeffel, 2009; Plainis, Petratou, Giannakopoulou, Atchison, & Tsilimbaris, 2011; Rajavi et al., 2015). The magnocellular pathway is important in the evaluation of stimulus depth (Hubel & Livingstone, 1987; Markó, Mikó-Barath, Kiss, Török, & Jandó, 2012) and motion information, including stimulus detection and CFF (S. G. Solomon, Martin, White, Rüttiger, & Lee, 2002). It determines contrast sensitivity for low spatial and high temporal frequency achromatic targets (Plainis & Murray, 2005) and plays a significant role in contrast adaptation (S. G. Solomon, Peirce, Dhruv, & Lennie, 2004). In addition, the magnocellular pathway signals are primarily located within the peripheral retina (Wen et al., 2015), which is thought to be important in emmetropization (Smith, 2013). Conversely, magnocellular differences in myopia may simply be a consequence of ocular elongation (Vera-Diaz et al., 2005). Coarse binocularity for gross disparity levels (Thompson & Wood, 1993) is independent from the high-acuity parvocellular disparity system. Indeed, results from evoked visual potentials of dynamic random-dot correlograms suggest that binocular correlation-processing cortical neurons receive predominantly magnocellular input (Markó et al., 2012). However, further work is necessary to relate potential myopic deficits in magnocellular processing to our findings pointing to a temporal-frequency dependent increase in stereopsis thresholds.

Together, our results point to temporal and spatial frequency–dependent differences in performance on binocular tasks between individuals with emmetropia and myopia, which may be a cause or consequence of structural changes that occur during emmetropization. Further investigation is needed to examine how these changes interact with other factors in the development of myopia, such as the amount of time spent performing near vision tasks as well as variability in accommodation state and consequent defocus. Our group has recently shown that individuals with myopia have more variable accommodation responses than emmetropes (Maiello, Kerber, Thorn, Bex, & Vera-Diaz, 2018). The relationship between spatiotemporal visual sensitivity and environmental factors in eye growth also warrants further research as animal models show a significant effect of the temporal modulation of light in axial elongation and the development of induced myopia (Crewther, Barutchu, Murphy, & Crewther, 2006; Di, Liu, Chu, Zhou, & Zhou, 2013; Lan, Feldkaemper, & Schaeffel, 2014; Rucker et al., 2015).

Keywords: myopia, binocularity, stereopsis, suppression, temporal frequency

Supplementary Material

Supplementary Movie S1. Example stereopsis threshold measurement chart with 4 Hz counterphase flicker. Each triplet has one randomly selected front-depth circle and two randomly selected back-depth circles. Designed for viewing with red–cyan anaglyph glasses.

Supplementary Movie S2. Example binocular balance chart with 4 Hz counterphase flicker. Different letters are shown to each eye, and the peak contrast of the two letters sums to 100%. Designed for viewing with red–cyan anaglyph glasses.

Acknowledgments

Adriana Ferreira was supported by an NEI T35 EY007149 grant to the New England College of Optometry; Anna Kosovicheva and Peter J. Bex were supported in part by NIH grants R01EY021553 (PB) and F32 EY028814 (AK); additional support was provided by the New England College of Optometry.

Commercial relationships: Prevention and Treatment of Myopia, Patent Application US20160212404 A1, PCT/US2014/052398 (PB, FVD).

Corresponding author: Fuensanta A. Vera-Diaz.
Email: Vera_DiazF@neco.edu.
Address: New England College of Optometry, Boston, MA, USA.

References

Banks, M. S. (1982). The development of spatial and temporal contrast sensitivity. *Current Eye Research*, *2*(3), 191–198.

Birch, E. E., Morale, S. E., Jost, R. M., De La Cruz, A., Kelly, K. R., Wang, Y.-Z., & Bex, P. J. (2016). Assessing suppression in amblyopic children with a dichoptic eye chart. *Investigative Ophthalmology and Visual Science*, *57*(13), 5649–5654.

Blake, R., & Rush, C. (1980). Temporal properties of binocular mechanisms in the human visual system. *Experimental Brain Research*, *38*(3), 333–340.

Brainard, D. H. (1997). The Psychophysics Toolbox. *Spatial Vision*, *10*(4), 433–436.

Burton, G. J., & Moorhead, I. R. (1987). Color and spatial structure in natural scenes. *Applied Optics*, *26*(1), 157–170.

Cavonius, C. R. (1979). Binocular interactions in flicker. *The Quarterly Journal of Experimental Psychology*, *31*(2), 273–280.

Chen, P. C., Woung, L. C., & Yang, C. F. (2000). Modulation transfer function and critical flicker frequency in high-myopia patients. *Journal of the Formosan Medical Association*, *99*(1), 45–48.

Comerford, J. P., Thorn, F., & Corwin, T. R. (1987). Effect of luminance level on contrast sensitivity in myopia. *American Journal of Optometry and Physiological Optics*, *64*(11), 810–814.

Crewther, S. G., Barutchu, A., Murphy, M. J., & Crewther, D. P. (2006). Low frequency temporal modulation of light promotes a myopic shift in refractive compensation to all spectacle lenses. *Experimental Eye Research*, *83*(2), 322–328.

Di, Y., Liu, R., Chu, R.-Y., Zhou, X.-T., & Zhou, X.-D. (2013). Myopia induced by flickering light in guinea pigs: A detailed assessment on susceptibility of different frequencies. *International Journal of Ophthalmology*, *6*(2), 115–119.

Dobkins, K. R., Anderson, C. M., & Lia, B. (1999). Infant temporal contrast sensitivity functions (tCSFs) mature earlier for luminance than for chromatic stimuli: Evidence for precocious magnocellular development? *Vision Research*, *39*(19), 3223–3239.

Ellemberg, D., Lewis, T. L., Liu, C. H., & Maurer, D. (1999). Development of spatial and temporal vision during childhood. *Vision Research*, *39*(14), 2325–2333.

Fahle, M. (1982). Binocular rivalry: Suppression depends on orientation and spatial frequency. *Vision Research*, *22*(7), 787–800.

Fahle, M. (1983). Non-fusable stimuli and the role of binocular inhibition in normal and pathologic vision, especially strabismus. *Documenta Ophthalmologica*, *55*(4), 323–340.

Field, D. J. (1987). Relations between the statistics of natural images and the response properties of cortical cells. *Journal of the Optical Society of America A*, *4*(12), 2379–2394.

Goss, D. A., & Wickham, M. G. (1995). Retinal-image mediated ocular growth as a mechanism for juvenile onset myopia and for emmetropization. A literature review. *Documenta Ophthalmologica*, *90*(4), 341–375.

Han, S., & Alais, D. (2018). Strength of continuous flash suppression is optimal when target and masker modulation rates are matched. *Journal of Vision*, *18*(3):3, 1–14, https://doi.org/10.1167/18.3.3. [PubMed] [Article]

Han, S., Lunghi, C., & Alais, D. (2016). The temporal frequency tuning of continuous flash suppression reveals peak suppression at very low frequencies. *Scientific Reports*, *6*:35723.

Harrad, R. A., McKee, S. P., Blake, R., & Yang, Y. (1994). Binocular rivalry disrupts stereopsis. *Perception*, *23*(1), 15–28.

Hartmann, E. E., & Banks, M. S. (1992). Temporal contrast sensitivity in human infants. *Vision Research*, *32*(6), 1163–1168.

Hess, R. F., Schmid, K. L., Dumoulin, S. O., Field, D. J., & Brinkworth, D. R. (2006). What image properties regulate eye growth? *Current Biology*, *16*(7), 687–691.

Hochberg, J. (1964, September 18). Depth perception loss with local monocular suppression: A problem in the explanation of stereopsis. *Science*, *145*, 1334–1336.

Hoffman, D. M., & Banks, M. S. (2010). Focus information is used to interpret binocular images. *Journal of Vision*, *10*(5):13, 1–17, https://doi.org/10.1167/10.5.13. [PubMed] [Article]

Hubel, D. H., & Livingstone, M. S. (1987). Segregation of form, and stereopsis in primate. *Cell*, *7*, 3378–3415.

Julesz, B., & Miller, J. E. (1975). Independent spatial frequency tuned channels in binocular fusion and rivalry. *Perception*, *4*(2), 125–143.

Kane, D., Guan, P., & Banks, M. S. (2014). The limits of human stereopsis in space and time. *The Journal of Neuroscience*, *34*(4), 1397–1408.

Kaunitz, L. N., Fracasso, A., Skujevskis, M., & Melcher, D. (2014). Waves of visibility: Probing the depth of inter-ocular suppression with transient and sustained targets. *Frontiers in Psychology*, *5*:804.

Kelly, D. H. (1971). Theory of flicker and transient responses: II. *Journal of the Optical Society of America A*, *61*(5), 632–640.

Kleiner, M., Brainard, D., & Pelli, D. G. (2007). What's new in Psychtoolbox-3? *Perception 36 ECVP Abstract Supplement*, *36*(14), 1.

Kretzmer, E. R. (1952). Statistics of television signals. *Bell System Technical Journal*, *31*(4), 751–763.

Kulp, M. T., Ying, G., Huang, J., Maguire, M., Quinn, G., Ciner, E. B., ... VIP Study Group. (2014). Associations between hyperopia and other vision and refractive error characteristics. *Optometry and Vision Science*, *91*(4), 383–389.

Kwon, M., Lu, Z.-L., Miller, A., Kazlas, M., Hunter, D. G., & Bex, P. J. (2014). Assessing binocular interaction in amblyopia and its clinical feasibility. *PLoS One*, *9*(6), e100156.

Kwon, M., Wiecek, E., Dakin, S. C., & Bex, P. J. (2015). Spatial-frequency dependent binocular imbalance in amblyopia. *Scientific Reports*, *5*(17181), 1–12.

Lan, W., Feldkaemper, M., & Schaeffel, F. (2014). Intermittent episodes of bright light suppress myopia in the chicken more than continuous bright light. *PLoS One*, *9*(10), e110906.

Lee, C. E., Lee, Y. C., & Lee, S.-Y. (2010). Factors influencing the prevalence of amblyopia in children with anisometropia. *Korean Journal of Ophthalmology*, *24*(4), 225–229.

Lee, S., Shioiri, S., & Yaguchi, H. (2003). Effects of temporal frequency and contrast on spatial frequency characteristics for disparity threshold. *Optical Review*, *10*(2), 120–123.

Lee, S., Shioiri, S., & Yaguchi, H. (2007). Stereo channels with different temporal frequency tunings. *Vision Research*, *47*(3), 289–297.

Maiello, G., Kerber, K. L., Thorn, F., Bex, P. J., & Vera-Diaz, F. A. (2018). Vergence driven accommodation with simulated disparity in myopia and emmetropia. *Experimental Eye Research*, *166*, 96–105.

Markó, K., Mikó-Barath, E., Kiss, H. J., Török, B., & Jandó, G. (2012). Effects of luminance on dynamic random-dot correlogram evoked visual potentials. *Perception*, *41*(6), 648–660.

Matin, L. (1962). Binocular summation at the absolute threshold of peripheral vision. *Journal of the Optical Society of America*, *52*, 1276–1286.

Nassi, J. J., & Callaway, E. M. (2009). Parallel processing strategies of the primate visual system. *Nature Reviews Neuroscience*, *10*(5), 360–372.

Nienborg, H., Bridge, H., Parker, A. J., & Cumming, B. G. (2005). Neuronal computation of disparity in V1 limits temporal resolution for detecting disparity modulation. *The Journal of Neuroscience*, *25*(44), 10207–10219.

Norcia, A. M., & Tyler, C. W. (1984). Temporal frequency limits for stereoscopic apparent motion processes. *Vision Research*, *24*(5), 395–401.

Ogle, K. N., & Wakefield, J. M. (1967). Stereoscopic depth and binocular rivalry. *Vision Research*, *7*, 89–98.

Ohlendorf, A., & Schaeffel, F. (2009). Contrast adaptation induced by defocus – A possible error signal for emmetropization? *Vision Research*, *49*(2), 249–256.

Ong, J., & Wong, T. (1971). Effect of ametropias on critical fusion frequency. *American Journal of Optometry and Archives of American Academy of Optometry*, *48*(9), 736–739.

Patterson, R. (1990). Spatiotemporal properties of stereoacuity. *Optometry and Vision Science*, *67*(2), 123–128.

Pelli, D. G. (1997). The VideoToolbox software for visual psychophysics: Transforming numbers into movies. *Spatial Vision*, *10*(4), 437–442.

Plainis, S., & Murray, I. J. (2005). Magnocellular channel subserves the human contrast-sensitivity function. *Perception*, *34*(8), 933–940.

Plainis, S., Petratou, D., Giannakopoulou, T., Atchison, D. A., & Tsilimbaris, M. K. (2011). Binocular summation improves performance to defocus-induced blur. *Investigative Ophthalmology and Visual Science*, *52*(5), 2784–2789.

Pointer, J. S. (2012). Sighting versus sensory ocular dominance. *Journal of Optometry*, *5*(2), 52–55.

Rajavi, Z., Sabbaghi, H., Baghini, A. S., Yaseri, M., Sheibani, K., & Norouzi, G. (2015). Prevalence of color vision deficiency and its correlation with amblyopia and refractive errors among primary school children. *Journal of Ophthalmic and Vision Research*, *10*(2), 130–138.

Richards, W. (1972). Response functions for sine- and square-wave modulations of disparity. *Journal of the Optical Society of America*, *62*(7), 907–911.

Robson, J. G. (1966). Spatial and temporal contrast-sensitivity functions of the visual system. *Journal of the Optical Society of America A*, *56*, 1141–1142.

Rucker, F., Britton, S., Spatcher, M., & Hanowsky, S. (2015). Blue light protects against temporal frequency sensitive refractive changes. *Investigative Ophthalmology and Visual Science*, *56*(10), 6121–6131.

Sanes, J. R., & Masland, R. H. (2015). The types of retinal ganglion cells: Current status and implications for neuronal classification. *Annual Review of Neuroscience*, *38*(1), 221–246.

Schor, C. M., & Wood, I. (1983). Disparity range for local stereopsis as a function of luminance spatial frequency. *Vision Research*, *23*(12), 1649–1654.

Schwahn, H. N., & Schaeffel, F. (1997). Flicker parameters are different for suppression of myopia and hyperopia. *Vision Research*, *37*(19), 2661–2673.

Shors, T. J., Wright, K., & Greene, E. (1992). Control of interocular suppression as a function of differential image blur. *Vision Research*, *32*(6), 1169–1175.

Smith, E. L., III (2013). Optical treatment strategies to slow myopia progression: Effects of the visual extent of the optical treatment zone. *Experimental Eye Research*, *114*, 77–88.

Smith, E. L., III, Hung, L.-F., & Arumugam, B. (2014). Visual regulation of refractive development: Insights from animal studies. *Eye*, *28*(2), 180–188.

Solomon, J. A., & Pelli, D. G. (1994, June 2). The visual filter mediating letter identification. *Nature*, *369*(6479), 395–397.

Solomon, S. G., Martin, P. R., White, A. J. R., Rüttiger, L., & Lee, B. B. (2002). Modulation sensitivity of ganglion cells in peripheral retina of macaque. *Vision Research*, *42*(27), 2893–2898.

Solomon, S. G., Peirce, J. W., Dhruv, N. T., & Lennie, P. (2004). Profound contrast adaptation early in the visual pathway. *Neuron*, *42*(1), 155–162.

Stavros, K. A., & Kiorpes, L. (2008). Behavioral measurement of temporal contrast sensitivity development in macaque monkeys (Macaca nemestrina). *Vision Research*, *48*(11), 1335–1344.

Thibos, L. N., & Horner, D. (2001). Power vector analysis of the optical outcome of refractive surgery. *Journal of Cataract and Refractive Surgery*, *27*(1), 80–85.

Thompson, P., & Wood, V. (1993). The Pulfrich pendulum phenomenon in stereoblind subjects. *Perception*, *22*(1), 7–14.

Thorn, F., & Boynton, R. M. (1974). Human binocular summation at absolute threshold. *Vision Research*, *14*(7), 445–458.

Tsuchiya, N., & Koch, C. (2005). Continuous flash suppression reduces negative afterimages. *Nature Neuroscience*, *8*(8), 1096–1101.

Tsuchiya, N., Koch, C., Gilroy, L. A., & Blake, R. (2006). Depth of interocular suppression associated with continuous flash suppression, flash suppression, and binocular rivalry. *Journal of Vision*, *6*(10): 6, 1068–1078, https://doi.org/10.1167/6.10.6. [PubMed] [Article]

Vera-Diaz, F. A., McGraw, P. V., Strang, N. C., & Whitaker, D. (2005). A psychophysical investigation of ocular expansion in human eyes. *Investigative Ophthalmology and Visual Science*, *46*(2), 758–763.

Wallman, J., & Winawer, J. (2004). Homeostasis of eye growth and the question of myopia. *Neuron*, *43*(4), 447–468.

Walls, G. L. (1951). A theory of ocular dominance. *Archives of Ophthalmology*, *45*(4), 387–412.

Watson, A. B., & Pelli, D. G. (1983). QUEST: A Bayesian adaptive psychometric method. *Perception and Psychophysics*, *33*(2), 113–120.

Weakley, D. R. (2001). The association between nonstrabismic anisometropia, amblyopia, and subnormal binocularity. *Ophthalmology*, *108*(1), 163–171.

Wen, W., Zhang, P., Liu, T., Zhang, T., Gao, J., Sun, X., & He, S. (2015). A novel motion-on-color paradigm for isolating magnocellular pathway function in preperimetric glaucoma. *Investigative Ophthalmology and Visual Science*, *56*(8), 4439–4446.

Westheimer, G., & McKee, S. P. (1980). Stereoscopic acuity with defocused and spatially filtered retinal images. *Journal of the Optical Society of America*, *70*(7), 772–778.

Yang, Y., & Blake, R. (1991). Spatial frequency tuning of human stereopsis. *Vision Research*, *31*(7–8), 1177–1189.

Zhi, Z., Pan, M., Xie, R., Xiong, S., Zhou, X., & Qu, J. (2013). The effect of temporal and spatial stimuli on the refractive status of guinea pigs following natural emmetropization. *Investigative Ophthalmology and Visual Science*, *54*(1), 890–897.

Zhu, W., Drewes, J., & Melcher, D. (2016). Time for awareness: The influence of temporal properties of the mask on continuous flash suppression effectiveness. *PLoS One*, *11*(7), e0159206.

Zhu, X., McBrien, N. A., Smith, E. L., Troilo, D., & Wallman, J. (2013). Eyes in various species can shorten to compensate for myopic defocus. *Investigative Ophthalmology and Visual Science*, *54*(4), 2634–2644.